`*JAREE* (year), page no
doi: 10.12962/jaree.xyzxyz

JAREE Journal on Advanced Research in Electrical Engineering
ISSN: 2579-6216

RESEARCH ARTICLE

The Governor Predictive Controlled Based on LSTM for Optimizing Cofiring Power Generator Operation

Addien Wahyu Wiranata[1], Dimas Anton Asfani*, and Daniar Fahmi

[1] Department of Electrical Engineering, Institut Teknologi Sepuluh Nopember, Surabaya, Indonesia

*Corresponding author (anton@ee.its.ac.id)

Received: 16 June 2025; **Revised:** 17 July 2025; **Accepted:** 18 July 2025

Abstract

The renewable energy with cofiring technology has a significant impact on the use of Biomass. The use of biomass with different qualities greatly affects the performance of a plant. Deep Learning Time Series Forecasting is designed for predicting two control parameters cofiring powerplant operation consist of governor control and output generator. Long Short-Term Memory (LSTM) combined with Multilayer Perceptron, Convolutional, and Adaptive Moment Estimation (ADAM) optimizer algorithms are utilized to optimize the process governor control and predict generating power output. Correlation analysis is used to determine the input variables and resulting input parameters of governor control prediction consist of Temperature Steam (°C), Pressure Steam (Psig), Output Generator (kW), Coal Flow (ton/hour), Flow Steam (m^3/hour). Moreover, the input variable for prediction generation power output are steam flow, steam temperature, coal flow, and steam pressure. The combination of Deep Learning Forecasting is successfully to predict both operation parameter percentage errors of 5.33%.

Keywords: cofiring technology, correlation coefficient, deep learning, long short term memory, RMSE

I. Introduction

The increasing number of cofiring uses in Steam Power Plants in various types, namely the Stoker type, CFB (Circulated Fluidized Bed), PC (Pulverized Coal). Biomass co-firing is recognized as an important technology to help reduce the use of fossil fuels, especially due to its relatively easy application with the characterization and conversion of energy that has key fuel properties, both chemical and thermochemical as well as energy conversion techniques focused on the implications of biomass co-firing are discussed along with an overview of current co-firing technologies[1]. The target energy mix from New & Renewable Energy (NRE) is 23% by 2025, Indonesia electricity Company, called Perusahaan Listrik Negara (PLN) plans to utilize more biomass-based fuels to be used jointly (co-firing) with coal in CFB (Circulated Fluidized Bed), PC (Pulverized Coal), and Stocker type coal-fired power plants with a biomass percentage for PC type boiler coal-fired power plants of 6%, CFB 40% and Stoker 70%, so that the production capacity of NRE from co-firing can be obtained of

2.7 GW which requires biomass of up to 14 million tons per year (assumption CF 70%)[2]. The use of biomass in cofiring will affect the operating parameters, especially in boilers and turbines. Boiler heaters achieve the highest design efficiency during optimal loads at 85–95% rated power with the most efficient heat production and during operation, boilers are often switched on, switched off, or run below rated output, using a specific fuel so it is essential to maintain combustion stability[3]. Combustion of coal with biomass seems to be possible, this combustion has the potential to produce the release of heat energy that fluctuates due to differences in calorie content and density, thereby increasing the occurrence of ash clumping which causes problems in the boiler, which has an impact on the performance of the boiler as a whole and has an impact on the production of steam produced to drive the turbine blades[4]. The high use of cofiring causes the output of the generator and the opening of the governor to fluctuate due to changes in combustion in the boiler. Its utilization as a renewable biomass resource has shown great potential with empirical findings related to the co-combustion of solid biomass and coal fuels for power generation at biomass and coal co-combustion ratios (100:0, 85:15, 90:10, 95:5, and 0:100) tested to optimize combustion efficiency and generator output so that the best maximum test is 10%[5]. The effect on the combustion process in the coal-fired power plant combustion chamber was tested using the parameters of ignition temperature, combustion temperature, and calorific value of the mixture (3500-4800 kcal) of the fuel, thus showing a strong indication of positive synergy in the mixing of several biomasses and practically no decrease in power with the biomass content in the fuel mixture reaching 30%[6]. Turbine models for dynamic stability in the regulation of frequency, pressure, and temperature of steam in constant conditions in each part due to the unlimited supply of steam because by opening the control valve can increase the steam discharge without reducing the quality of the steam but in reality the steam is supplied by boilers that use coal, oil, natural gas, biomass, nuclear reactors, and dual fuels such as the combustion of more than one type of fuel so that the amount of steam is Produced may fluctuate[7].

The optimization of the governor opening as a reference point in response to the impact of cofiring utilization can be made as a learning data to provide an operation characteristic. The main driving mechanisms in the turbine-governor control model are generally classified into three types: (1) steam turbines, (2) hydraulic turbines, and (3) gas turbines for combined-cycle cogeneration plants[7]. All turbine-boiler control strategies including turbine control mode, boiler control, and deep learning-based control are also taken into account in the modelling procedure, so that the integrated model can be adapted for all

How to cite: Wiranata, A. W., Asfani, D. A., & Fahmi, D. (2026). The Governor Predictive Controlled Based on LSTM for Optimizing Cofiring Power Generator Operation. JAREE (Journal on Advanced Research in Electrical Engineering), Volume 10 (No.1).

steam units to increase the cofiring percentage by up to 100%[8]. Artificial intelligence and machine learning algorithms integrated with turbines and boilers can be useful in controlling important variables such as pressure, temperature, speed, and humidity so that comparisons show that the integration of artificial neural networks and electrical circuits shows performance improvements with high predictive accuracy at yield deviations of less than 1%[9]. The advantage of a properly tuned steam turbine governor with modifications to the control parameters is that it can provide effective damper torque at low-frequency oscillations in the power system so that the generator output power can be optimized[10]. The use of Deep Learning for Time Series learning methods to recognize various operating parameters during cofiring can maintain the efficiency of the plant's operation pattern in subsequent operations. Deep learning refers to machine learning techniques that use range and/or no-exploration strategies to automatically learn hierarchical

representations in deep architectures for the latest classifications and research inspired by an emphasis on the importance of variance in improving the functionality and efficiency of such algorithms, particularly in the field of dynamic deep learning for autocorrelation guided model construction and level optimizers Further points to a promising path for future research, offering the potential for more efficient and accurate deep-based learning[11],[12]. The use of deep learning provides optimization of the generator load output and opens the regulator above 70% capacity and with a short-term memory algorithm can serve as an estimator in the speed control function of the regulator's drop speed control to maintain the efficiency of the equipment[13].

The use of cofiring is very low due to the biomass factor so that it is difficult for Steam Power Plants to increase the use of cofiring above 5%, this is because the typical steam plant sourced from Coal has a higher calorific value and density than Coal so that the percentage of cofiring is difficult to increase which affects the condition of boilers and turbines. Cofiring as one of the sources of New Renewable Energy (NRE) has high potential to be developed where the energy potential from biomass (bioenergy) reaches 32.6 GW, with its utilization only reaching 1,895.7 MW or around 5.8%, this is also Indonesia's commitment in setting a target of achieving a renewable energy mix of 23% in 2025 and 31% in 2050 where cofiring is one of the things to be achieved[14]. The use of combustion substitution with cofiring in boilers with a mixture of 95% Coal and 5% Biomass did not have a significant difference, the results of the heat rate calculation by the input-output method showed that the Gross Plant Heat Rate of coal combustion was 2649 kcaI/kWh while the co- firing value was 2705 kcal/kWh, with a decrease in gross kWh production by 1% during co-firing and the Net Plant Heat Rate value at the time of cofiring was 2.25% higher than in when burning coal[15]. The impact of high cofiring will greatly affect the operating parameters so that it greatly affects operations by using coefficient-correlation as an attachment relationship. Analysing the correlation between features quantitatively and various validation criteria such as the square mean root error and the correlation coefficient (R) was used to validate the model, which

is a statistical measure that measures the strength and direction of the linear relationship between two variables ranging from -1 to +1, with -1 representing a perfect negative correlation, +1 a perfect positive correlation, and 0 no linear relationship[16],[17],[18]. The collection of performance test data as a test material for the implementation of cofiring is not able to justify the ideal percentage in maintaining the output of the generator and the governor opening.

Long Short Term Memory (LSTM) modelling will help in improving the prediction of generator output from the cofiring percentage parameters used. The use of the Long Short Term Memory (LSTM) deep learning algorithm outperforms conventional machine learning (ML) methods in terms of performance which suggests that deep learning strategies achieve higher classification accuracy by successfully learning complex patterns and representations in data and the high accuracy of LSTM (long short term memory) demonstrates its capacity to identify important characteristics and provide accurate predictions in context Specific tasks[19]. In addition, machine learning with long- short-term series modelling will also predict the output of the generator and the opening of the governor in the next few hours/days according to the date time used. LSTM will be combined with Multilayer Perceptron (MLP), Convolutional Neural Network (CNN), and Adam Optimizer. MLP is trained using input features to predict the reference values used as a model of the neuron network (or node) in a given layer associated with the neurons available in the previous layer and each connection has a unique strength or weight[20]. The convolutional operations found in CNN are performed directly in the graph domain, reducing computational complexity while minimizing the loss of structural information and as a result of extreme computing, the model has the best performance and is able to process reduced errors that can be attributed to the amount of information in the process[21]. The Adam optimizer is used to study temporal dependencies and extract feature error events with power exponential learning rate and is proposed as a controller of iteration direction and step size in solving local minimum problems, overshoots or oscillations caused by fixed values of learning rate during parameter updates[22]. Deep learning modelling aims to model the cofiring condition to maintain the performance of operating parameters, as a control function in maintaining the effectiveness of the governor opening and this modelling will later be used as an improvement in developing a governor system that is able to control other equipment to maintain performance when the cofiring program is carried out with a percentage scale of up to 100%.

II. Methods

Optimization of the use of cofiring on generator outputs and governor openings using Machine Learning and concept program methods will be used:

A. Grouping (%) of Cofiring Data Performance

Fig.1 explanation about percentage biomass that 0-3% Cofiring normal coal-fired power plant load conditions output generator more than 6000 kW with the use of corn cob biomass

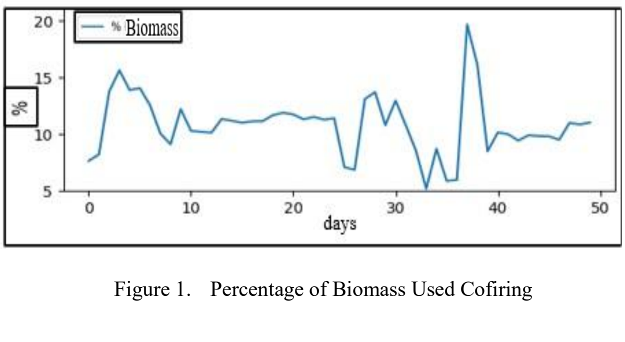

Figure 1. Percentage of Biomass Used Cofiring

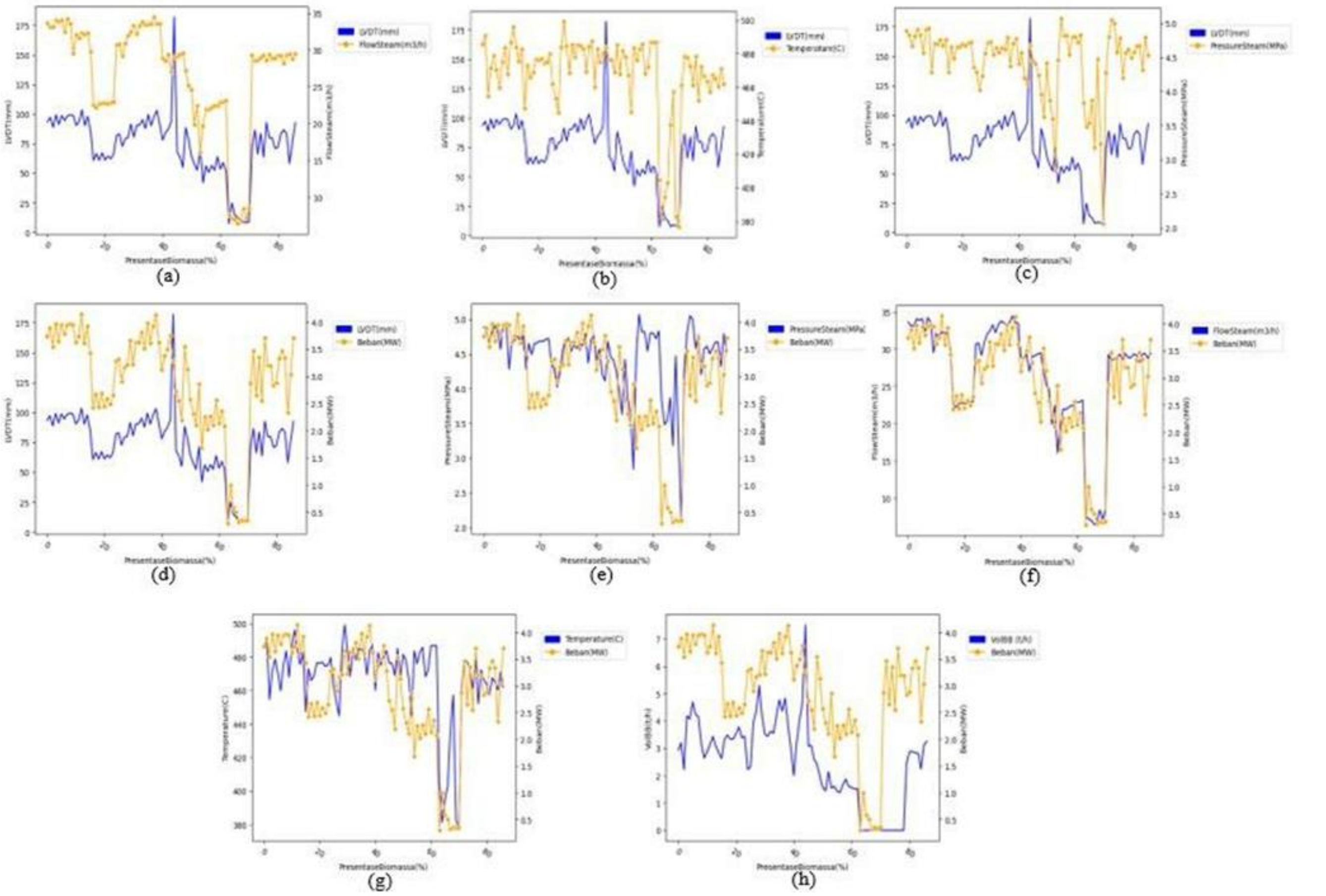

Figure 2. Correlation Graph (a)Governor-Flow Steam; (b)Governor-Temperature; (c)Governor-Pressure Steam; (d)Governor- Load; (e)Load-Pressure Steam; (f)Load-Flow Steam; (g)Load-Temperature; (h)Load-Biomass/Coal Volume

and woodchip. 5% Cofiring coal-fired power plant load conditions decreased with the use of corn cob biomass and woodchips at an average load of 4500 kW. 10- 50% Cofiring of unstable coal-fired power plant load conditions in 3000 kW, use of corn cob biomass and woodchip'100% Cofiring of coal-fired power plant load conditions less than 1000 kW, use of corn cob biomass and Woodchip.

10-50% Cofiring Temperature condition is at > 475°C but steam pressure does not rise and tends to drop. 100% Cofiring conditions Temperature and Pressure steam hunting are below the standard Pressure Steam less than 4.5 MPa, make impact on changes in output generator make fluctuate so that can disturb the grid system.

B. Mapping Data Input Program

Fig.1 shown shows eight figures 1(a)- (h) illustrating the relationship between various operational parameters and the percentage of cofiring. Fig.1(a) shows the relationship between the opening rate of the governor (mm) and the Flow Steam (m^3/h), both of which decrease significantly as the percentage of cofiring increases, suggesting the influence of steam flow on process performance. In Fig.1(b), the relationship between the governor's opening rate (mm) and temperature (°C) shows similar fluctuations, especially towards the end of the process, suggesting that temperature changes also affect the governor's opening rate (mm). Fig.1(c) shows the relationship between the opening rate of the governor (mm) and the pressure steam (Psig), with a corresponding pattern of decline, showing a potential direct relationship between pressure and cofiring efficiency. Furthermore, Fig.1(d) illustrates the correlation between the governor opening rate (mm) and the load (MW), where the decrease in system load is also followed by the decrease in the governor opening rate (mm), reflecting the correlation between power consumption and flow performance. Fig.1(e) shows the relationship between pressure steam (MPa) and load (MW), which shows that pressure drop correlates with load drop, showing the effect of pressure on the energy efficiency of the system. In Fig.1(f), the relationship between Flow Steam (m^3/h) and load (MW) is shown, with consistent fluctuations, which reinforces the conjecture that the rate of steam flow is highly dependent on the power requirements of the system. Fig.1(g) shows the relationship between temperature (°C) and load (MW), with a consistent pattern of decline, suggesting that changes in system temperature are closely related to operational load. Finally, Fig.1(h) shows the relationship between Biomass/Coal Volume (T) and load (MW), where Biomass/Coal Volume when load decreases can indicate improved system efficiency under low load conditions. Overall, the graph illustrates the close relationship between process parameters and system performance, especially in the context of percent cofiring and operating load.

The correlation analysis shown in table 1 supports the visual findings of Figure 1. The highest correlation coefficient was recorded in the relationship between the Output Generator and the Steam Flow of 0.93 (Fig.1(f)), and between the Governor and the Output Generator of 0.92 (Fig.1(d)), both of which were in the

"Very High" category. This shows that there is a very strong relationship between the system load and the flow and control parameters. The relationship between Governor and Flow Steam (Fig.1(a)) also showed a very high correlation of 0.85. Another high correlation was found in the relationship between Generator Output and Biomass/Coal Volume (Fig.1(h)) of 0.68, and between Generator Output and Steam Temperature (Fig.1(g)) of 0.62. Meanwhile, several parameters showed a moderate correlation, such as the relationship between Governor and Pressure Steam (Fig.1(c)) of 0.53, and Output Generator and Pressure Steam (Fig.1(e)) of 0.56. These results indicate that although some parameters such as steam pressure have a limited influence, most process parameters show a strong influence on system performance, especially those directly related to flow, temperature, and output power. So it can make decisions for control.

Table 1. Coefficient Correlation Scale

Fig.1	Main Parameter	Variable Parameter	Coefficient Correlation	Scale
(a)	Governor	Flow Steam	0.85	Very High
(b)	Governor	Temperature Steam	0.64	High
(c)	Governor	Pressure Steam	0.53	Moderate
(d)	Governor	Output Generator	0.92	Very High
(e)	Output Generator	Pressure Steam	0.56	Moderate
(f)	Output Generator	Flow Steam	0.93	Very High
(g)	Output Generator	Temperature Steam	0.62	High
(h)	Output Generator	Volume Biomass/Coal	0.68	High

C. *Formula Deep Learning Time Series Foreccasting*

Representation Formula Deep Learning Time Series Forecasting Method show in step 1 until 3;

Step 1 Multilayer Perceptron [23]:

$$y = f\ (x; \theta) \tag{1}$$

$$h_1 = \sigma(W_1 x + b_1) \tag{2}$$

$$h_1 = \sigma(W_{l-1} h_{l-1} + b_1) \tag{3}$$

$$CE(f(x; \theta, y) = -y^T \log (f\ (x; \theta)) \tag{4}$$

The classification model is defined in the link function (f) by connecting the input vector (x) and the output vector (y) where for all MLP layers, (f) consists of a number of transformations with (θ) representing all parameters of the Multilayer Perceptron including weight (W) and bias (b), and (σ) is used as a clock-like activation function.

Step 2 Convolutional Neural Networks [24],[25],[26],[27]:

$$w_{out} = \left\lceil \frac{w_{in} - e + 2p}{s} \right\rceil + 1 \tag{5}$$

$$h_{out} = \left\lceil \frac{h_{in} - e + 2p}{s} \right\rceil + 1 \tag{6}$$

$$d_{out} = k \tag{7}$$

Convolutional representations of width (w_{in}), height (h_{in}), depth (d_{in}), zero padding (p) and this volume is processed by a total filter (k) representing the weight of the connection in a convolutional network with a number of hyperparameters to produce the output volume.

Step 3 Long Short-Term Memory [24],[25],[26],[27],[28]:

$$i_t = \sigma(x_t U^i + h_{t-1} W^i) \tag{8}$$

$$f_t = \sigma(x_t U^f + h_{t-1} W^f) \tag{9}$$

$$o_t = \sigma(x_t U^o + h_{t-1} W^o) \tag{10}$$

$$\tilde{C}_t = \tanh(x_t U^g + h_{t-1} W^g) \tag{11}$$

$$\tilde{C}_t = \sigma(f_t * C_t + i_t * \tilde{C}_t) \tag{12}$$

$$h_t = \tanh\ (C_t) * o_t \tag{13}$$

The algorithm considers each gate where (i_t) and (o_t) refer to the input gate, forget it, output gate, respectively at time (t). While (x_t) and (h_t) refer to the number of input features as well as the number of hidden units, respectively. (W) and (U) are weights matrix adjusted during learning along with (which is a bias where the initial values are ($c_o = 0$) and ($h_o = 0$) and all gates have the same dimension, the size of the hidden state ($\tilde{C}_t$) is the hidden state of the "candidate", (C_t) is the internal memory of the unit.

D. *Running Program Algorithm Deep Learning*

The initial stage starts from the data processing process (preprocessing) Fig.3, where operational parameters such as the speed of opening the governor, steam flow and temperature, and generator output load are prepared as input models. This data is classified into two main groups based on the modeling objectives, namely:

a. Control: Parameters used to set the system directly, such as the speed of opening the governor and the speed of operation of the coal feeder.
b. Predictive target: The output parameters that are the target of the model's prediction include the generator power output > 70%, the main steam pressure > 4.5 MPa, and the steam temperature > 450°C.

The Multilayer Perceptron (MLP) algorithm Fig.3 is a type of feedforward artificial neural network that is used in the preliminary stages to filter input data. This algorithm does not consider the sequence of time in the data, so it is used for the extraction of the initial features [23]. The output of the MLP becomes a vector representation of the feature that will be further processed by CNN and LSTM. Convolutional Neural Network (CNN) algorithms Fig.3 is used to detect local patterns between time steps. The CNN model consists of a convolutional layer and a max collection that generates a feature map. The map is flattened and processed by a solid layer to produce predictions. CNN in this context plays a significant role in recognizing spatial correlations in operational data sequences [24],[25],[26],[27],[28].

The Long Short-Term Memory (LSTM) algorithm Fig.3 is a type of Recurrent Neural Network (RNN) designed to deal with the problem of gradient disappearing in long- sequence data. In this system, LSTMs read inputs sequentially and learn from the long-term patterns contained in the data. This model is particularly effective in recognizing complex and non-linear temporal relationships in the operational data of generation. The combination of Deep Learning for Time Series Forecasting combines the power of MLP, CNN, and LSTM synergistically.

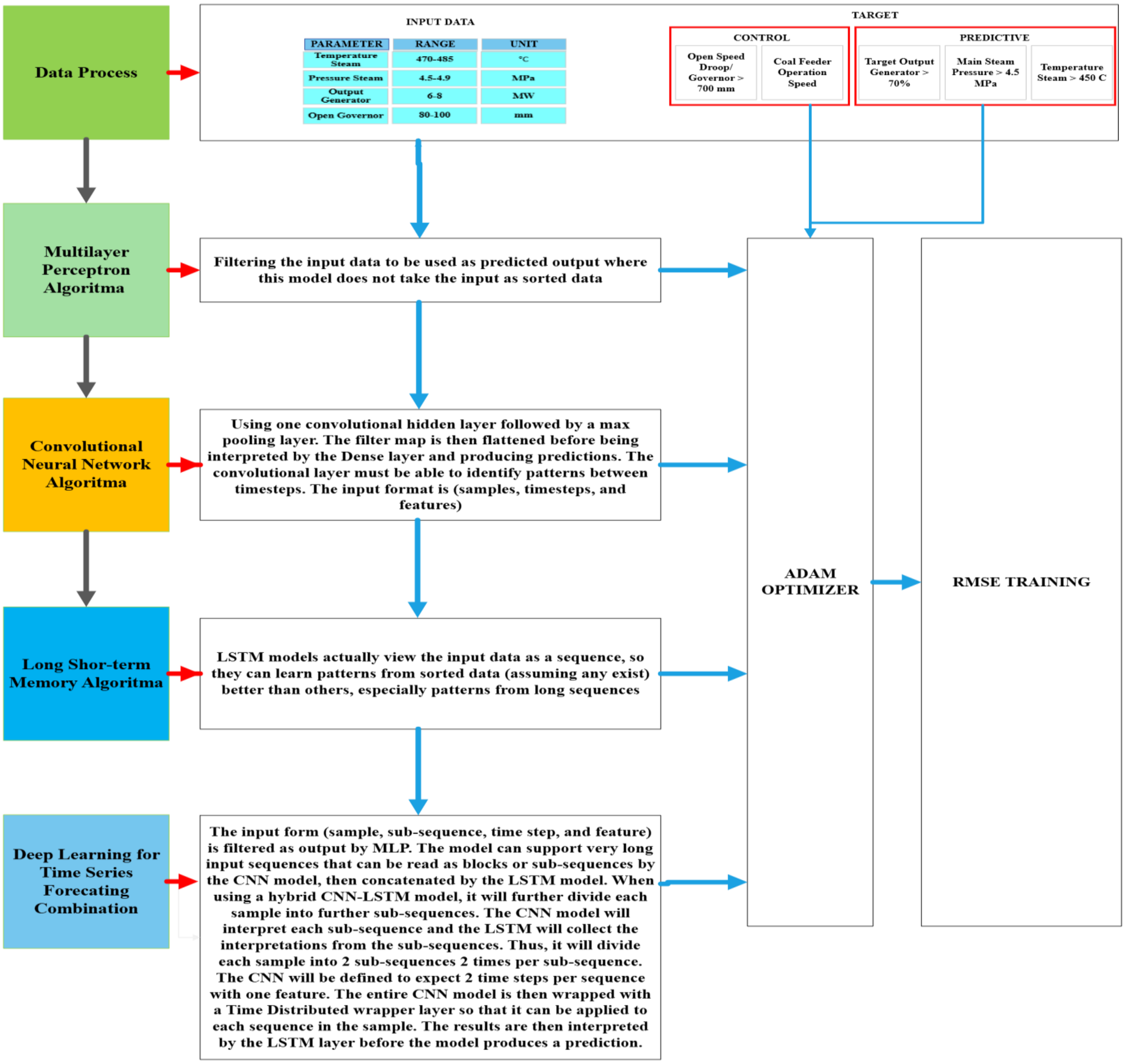

Figure 3. Deep Learning Time Series Forecasting Process System

The data input is formatted in form (sample, sub-sequence, step time, feature) and then filtered through MLP. Then the data is divided into CNN-recognizable sub-sequences. The output from the CNN will be further processed by the LSTM to capture temporal dynamics. This hybrid model allows for simultaneous learning of spatial and temporal features, improving prediction accuracy compared to an individual use of a single model [24],[25],[26],[27].

Optimization and Evaluation The model is carried out using an ADAM (Adaptive Moment Estimation) optimization algorithm which is efficient in accelerating convergence and overcoming non-stationary problems in the data. Model performance evaluation was performed using the Root Mean Square Error (RMSE) metric, which provides a measure of prediction error to the actual value in the training and relationship engagement phases using correlation coefficients [24],[26],[27],[29].

E. *Validation Root Mean Square Error (RMSE) and Coefficient Correlation*

RMSE ensures that total squared errors are minimized during training, which promotes model convergence [30]. The RMSE of the improved algorithmic model is significantly reduced and evaluated which is widely used for time series forecasting.

$$RMSE = \sqrt{\frac{1}{T}\sum_{t=1}^{T}(y_t - \hat{y}_t)^2} \tag{14}$$

$$SEM = SD\sqrt{1-r} \tag{15}$$

Where, $\hat{y}_t$ and y_t each represent the approximate value and the actual value [29]. The standard measurement error (SEM) for each session is calculated as follows where SD is the standard deviation of the session and r is the retest of the correlation coefficient [31].

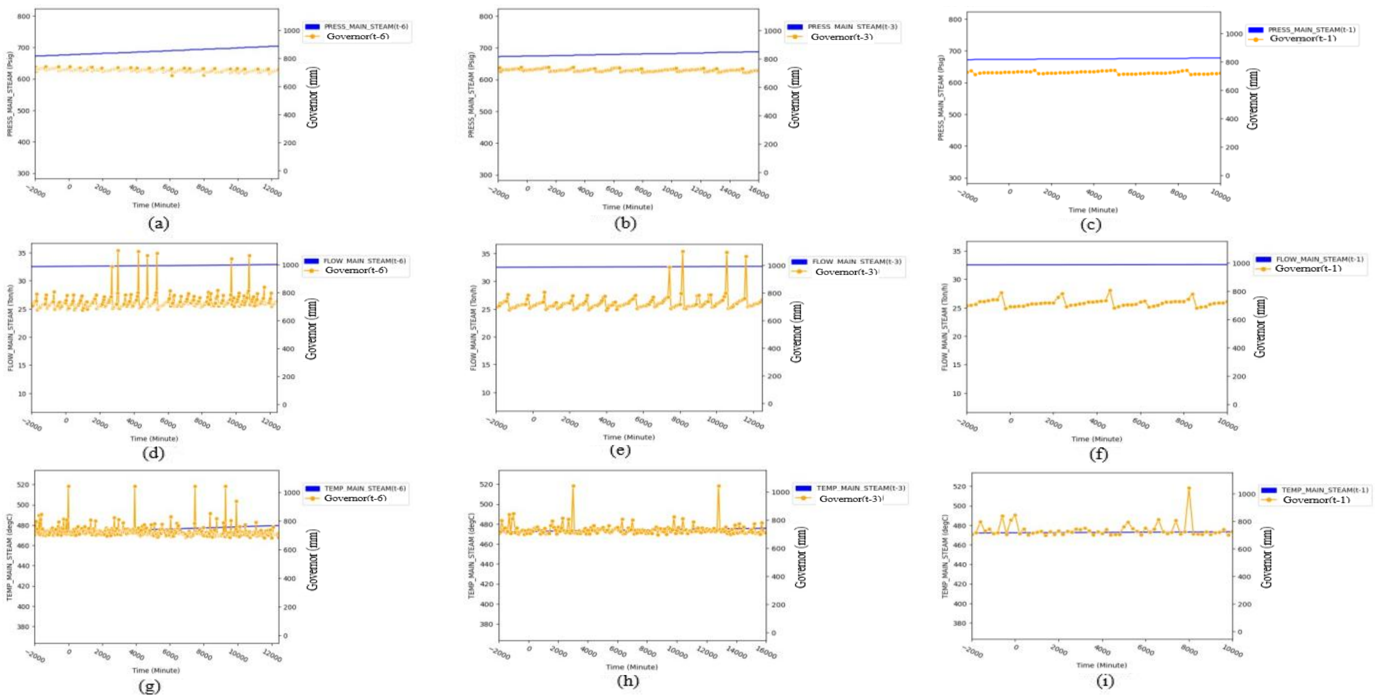

Figure 4. Prediction Performance (a) Governor-Pressure Steam(T-6); (b) Governor-Pressure Steam(T-3); (c) Governor-Pressure Steam(T-1); (d) Governor-Flow Steam(T-6); (e) Governor-Flow Steam(T-3); (f) Governor-Flow Steam(T-1); (g) Governor- Temperature Steam(T-6); (h) Governor-Temperature Steam(T-3); (i) Governor-Temperature Steam(T-1)

III. RESULTS AND DISCUSSION

Results were analyzed based on the pairing of control and prediction parameters with correlation coefficient values at the previous four time points: T-12 (twelve hours), T-6 (six hours), T-3 (three hours), and T-1 (one hour). And show the graph correlation forecasting just for T-6 (six hours), T-3 (three hours), and T-1 (one hour). The interpretation of the correlation is based on a standard scale, with a value of >0.8 categorized as "Very High", 0.6-0.8 as "High", and so on. The focus is to identify which parameters have the most significant influence on other variables in near real- time[16],[17],[18]. In addition to reflecting the model's generalization capabilities, validation data is used by calculating the error percentage of the Root Mean Square Error (RMSE) value.

A. Governor Control Prediction Performance (T-12; T-6; T-3;T-1)

Analysis of the prediction performance between the main parameters of the steam system (steam pressure, steam flow and steam temperature) to the governor openings the analysis was carried out based on nine graph images (a–i) that visualized the data over the time spans (T-6), (T-3), and (T- 1). In Fig.4 graphs (a), (b), and (c), the main pressure of the steam (shown in blue) increases gradually but consistently over time. Meanwhile, the governor's aperture (orange colour) tends to be stable with little fluctuation. This suggests that changes in steam pressure do not directly trigger significant changes in the governor's opening. The analysed data consisted of a pair of control and prediction parameters with correlation coefficient values at table 2 the previous three time points, namely: 0.576; 0.592; and 0.645. Fig. 4 Graphs (d), (e), and (f) show that the main flow of steam remains stable around the maximum number on the graph scale. In contrast, the governor's opening is subject to large and recurring fluctuations, with sharp peaks appearing periodically. This phenomenon indicates that the control system is actively adjusting to certain demands or conditions, even though the flow rate is maintained at an optimal level The analysed data consists of a pair of control and prediction parameters with correlation coefficient values at table 2 the previous three time points, namely: 0.005; 0.416; and 0.914.

Fig.4 Graphs (g), (h), and (i) show that the main temperature of the steam is very stable in the range of 500 °C. Meanwhile, the governor's opening experienced moderate to high fluctuations, with some sharp spikes, especially on graphs (g) and (i). Temperature stability despite variable aperture indicates efficiency in heat control. The analysed data consisted of a pair of control and prediction parameters with correlation coefficient values at table 2 the previous three time points, namely: -0.414; -0.552; and -0.841.

B. Output Generator Prediction Performance (T-12; T-6;T-3;T-1)

In a steam turbine-based power generation system, the output of the electrical power produced is greatly influenced by key parameters such as pressure, flow, and temperature of the main steam. The purpose of this report is to analyze the relationship of these three parameters with generator output to understand the influence of each on the performance of the generating system. Fig. 5 Graphs (a), (b), and (c) show the prediction performance between the main steam pressure and the generator output on several datasets. The steam pressure (shown on the blue line) tends to be stable with a slight increase, while the output of the generator (orange line) maintains stability in the range of 7000 to 7500 kW.

Table 2. Coefficient Correlation Control and Prediction Target

Main Parameter	**Variable Parameter**	**Coefficient Correlation**				**Scale**
		T-12	T-6	T-3	T-1	
Governor (c)	Flow Steam (p)	0.522	0.576	0.592	0.645	High
Governor (c)	Temperature Steam (p)	0.000	0.005	0.416	0.914	Very High
Governor (c)	Pressure Steam (p)	-0.483	-0.414	-0.552	-0.841	Very High
Governor (c)	Output Generator (p)	0.000	0.020	0.553	0.817	Very High
Governor (c)	Coal Flow (c)	0.122	0.614	0.739	0.937	Very High
Output Generator (p)	Flow Steam (p)	0.078	0.347	0.312	0.920	Very High
Output Generator (p)	Temperature Steam (p)	0.478	0.303	0.511	0.901	Very High
Output Generator (p)	Pressure Steam (p)	0.018	-0.044	-0.499	-0.719	High
Output Generator (p)	Coal Flow (c)	0.140	0.982	0.612	0.830	Very High
(c): Control Target (p): Prediction Target						

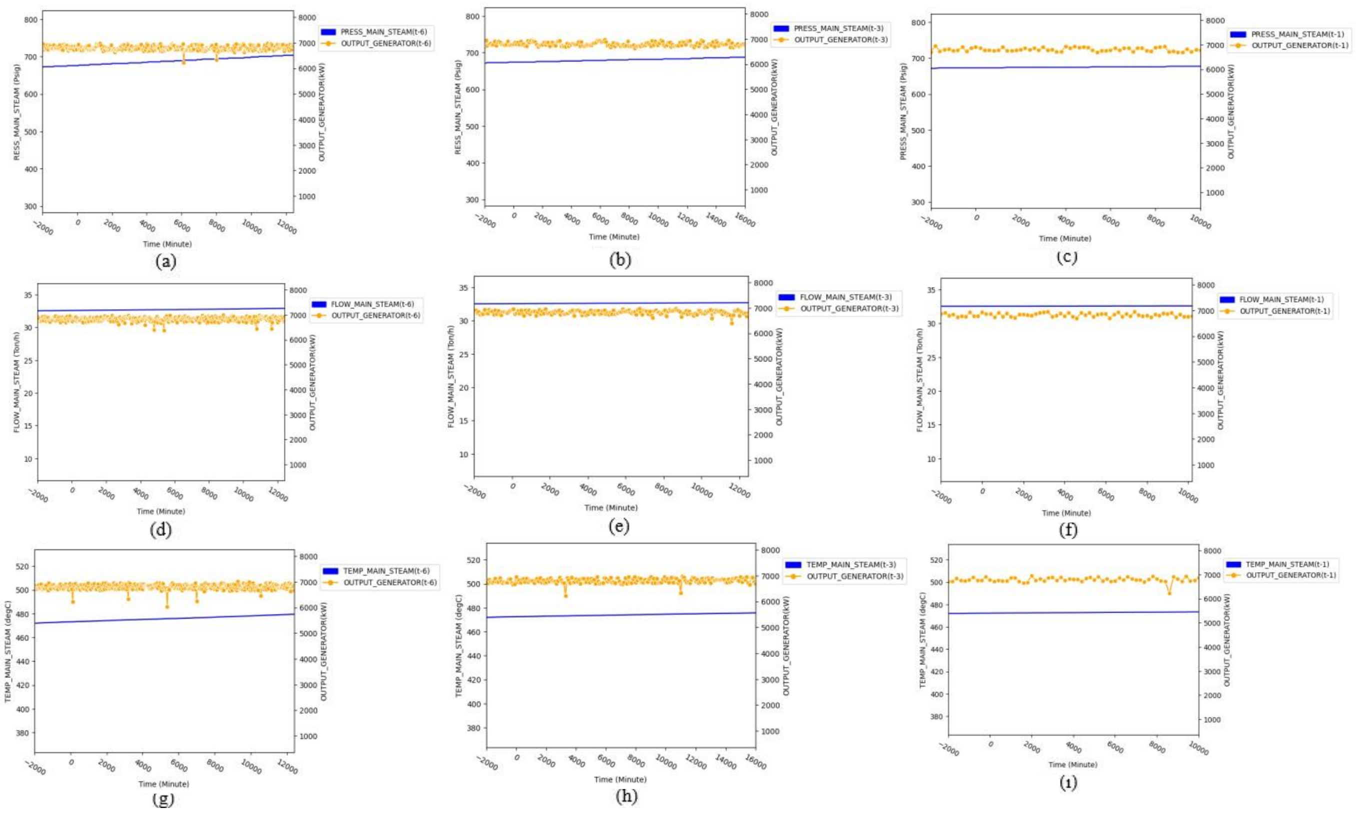

Figure 5. Prediction Performance (a)Generator-Pressure Steam(T-6); (b)Generator -Pressure Steam(T-3); (c)Generator - Pressure Steam(T-1); (d)Generator - Flow Steam(T-6); (e)Generator -Flow Steam(T-3); (f)Generator -Flow Steam(T-1); (g) Generator -Temperature Steam(T-6); (h) Generator -Temperature Steam(T-3); (i) Generator -Temperature Steam(T-1)

This indicates that the power output is directly affected by small pressure variations. The analyses data consisted of a pair of control and prediction parameters with correlation coefficient values at table 2 the previous three time points, namely: -0.044; -0.499; and -0.719. Fig. 5 Graphs (d), (e), and (f) show the relationship between the main steam flow and the generator output. The steam flow shows high stability in the range of 27-30 tons/h. The output of the generator set also remains consistently high. This stability shows a strong positive correlation, where the increase and stability of steam flow is related to the output power performance. This parameter seems to be the dominant factor in maintaining optimal generator output.

The analyzed data consisted of a pair of control and prediction parameters with correlation coefficient values at table 4 the previous three time points, namely: 0.347; 0.312; and 0.920. Fig. 5 Graphs (g), (h), and (i) show the main temperatures of the steam which tend to rise slowly over time, although there are slight fluctuations at some points. The output of the generator remains in the high range and is stable. The correlation between temperature and generator output appears to be positive where the temperature rise plays a role in generation efficiency. The analysed data consisted of a pair of control and prediction parameters with correlation coefficient values at table 4 the previous three time points, namely: 0.347; 0.312; and 0.920.

C. Coal/Biomass Flow Control Prediction Performance (T-12;T-6; T-3;T-1)

Fig. 6 Graphs (a), (b), and (c) show the prediction performance between the opening of the governor and the output of the generator on T-6; T-3; and T-1. The opening of the governor (orange line) has large fluctuations with repeated sharp spikes, while the output of the generator (blue line) is relatively stable in the range of 7000-8000 kW. This shows that the governor control system is actively adjusting the steam flow to maintain the stability of the output power, even though the aperture fluctuations are very dynamic. The analyzed data consisted of a pair of control and prediction parameters with correlation coefficient values at table 4 the previous three points, namely:0.020; 0.553; and 0.817. In Fig. 6 graphs (d), (e), and (f), the relationship between coal flows and governor openings for each of the same units is shown, coal flow (blue line) shows a tendency to increase slowly but steadily, while the governor openings still show a spike reflecting a dynamic response to system load. This signifies that combustion control is set to respond to power requirements through fuel flow regulation and

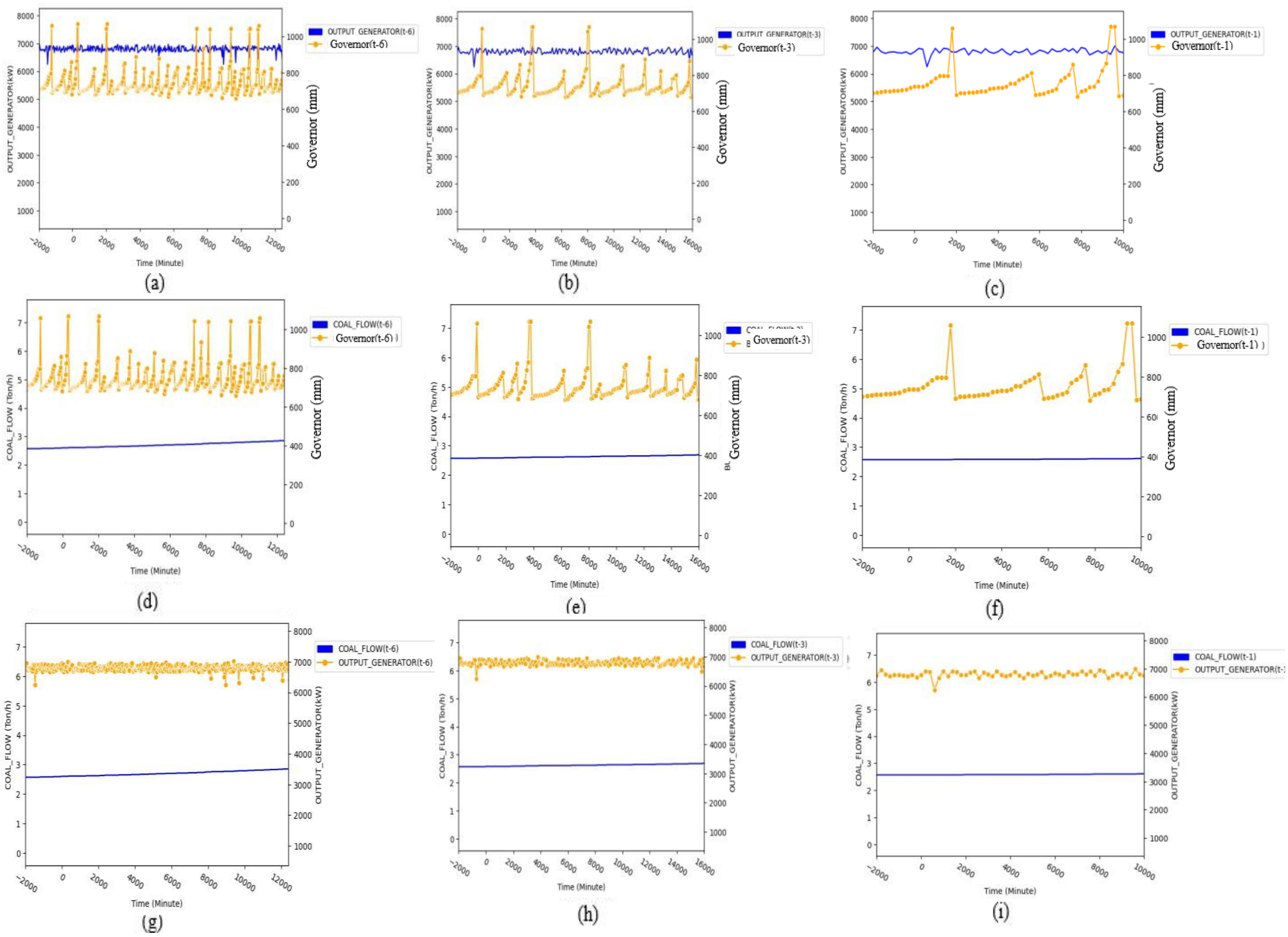

Figure 6. Prediction Performance (a)Generator-Governor(T-6); (b)Generator -Governor(T-3); (c)Generator -Governor(T-1); (d)Coal Flow-Governor(T-6); (e) Coal Flow-Governor (T-3); (f) Coal Flow-Governor (T-1); (g)Generator -Coal Flow(T-6); (h)Generator -Coal Flow (T-3); (i)Generator -Coal Flow (T-1)

valve openings. The data analyzed consisted of a pair of control and prediction parameters with correlation coefficient values at table 4 the previous three points, namely: 0.614; 0.739;and 0.937. Fig. 6 Graphs (g), (h), and (i) show the relationship between the coal flow and the generator output here, the coal flow shows good stability with slow increase, and the generator output remains in the high range without large fluctuations. This shows that the increase in coal flow is directly proportional to the stability of power output, so it can be concluded that a stable fuel supply is a key factor in maintaining optimal generator power output. Overall, the data showed that despite the aggressive changes in the opening of the regulator, the system was still able to keep the generator output in a stable condition, thanks to the integrated control between the coal flow and the feeder valve response. The generation system shows responsive performance yet remains efficient against fluctuations in load demand. The data analyzed consisted of a pair of control and prediction parameters with correlation coefficient values at the previous three times, namely: 0.382; 0.612; and 0.830.

D. Validation Root Mean Square Error (RMSE)

Based on the performance evaluation results of the four machine learning model architectures tested in table. 3, namely MLP, CNN, LSTM, and the combined DL-TSF (MLP-CNN-LSTM), it can be concluded that the combined - DL-TSF model provides the best overall results.

Table 3. Root Mean Square Error (RMSE) Process

Model	Parameter	Train RMSE	Validation RMSE	Error (%)
MLP	1001	585,8	667,2	12,2
CNN	9893	994,2	1109,1	10,4
LSTM	10451	969,0	1025,0	5,5
DL-TSF	**35979**	**984,8**	**1040,3**	**5,3**

Although this model has the highest number of parameters, at 35,979, which reflects the higher complexity of the architecture, its performance shows advantages in terms of accuracy and generalization capabilities. This is demonstrated by an RMSE validation value of 1040.3 and a lowest error percentage of 5.3%, outperforming single models such as MLP, CNN, and LSTM. So, it has a small error when used as a control function in the program process.

IV. Conclusion

Overall conclusions, the main vapor pressure, flow, and temperature parameters show good stability during the monitoring period, while the governor openings indicate active dynamics in the system. This indicates that the governor control system works to maintain the turbine's operating stability despite slight variations in load or operating conditions. The correlation between the main parameters of steam and the governor opening tends to be weak, which could indicate the presence of efficient automatic control in the system. Based on the analysis of the nine graphs, it can be concluded that the output of the generator is most affected by the stability of the main steam flow, while pressure and temperature contribute a smaller additional contribution. The generating system shows high efficiency with excellent electrical output stability, indicating optimal system control settings. Monitoring and controlling flow parameters should remain the focus in maintaining generation performance.

Analysis obtained showed that the Governor as a control parameter had a very high correlation with Steam Temperature (0.914), Steam Pressure (-0.841), Generator Output (0.817), and Coal Flow (0.937) at T-1 time. The relationship with Flow Steam was also relatively high (0.645), although not as strong as the other variables. These values suggest that the change in the Governor greatly affects the prediction parameters, especially near real-time (T-1). Meanwhile, the Generator Output as a control parameter also showed a very high correlation with Steam Flow (0.920), Steam Temperature (0.901), and Coal Flow (0.830) at T-1 time. A significant negative correlation (- 0.719) was also found between the Output Generator and Steam Pressure, indicating an inverse relationship between these two variables. In general, the highest correlation appears at the time of T-1, which suggests that time-based prediction models are more accurate in predicting target variables. The interpretive scale shows that most relationships are at "Very High" levels, reinforcing the importance of monitoring and controlling these parameters in real-time to improve the performance, efficiency, and stability of the generating system. This research can be used as the basis for the development of prediction-based control systems in the future. The RMSE validation of Deep Learning Time Series Forecasting 1040.3 and the error percentage of 5.3% is highly competitive in handling validation data and provides an optimal balance between model complexity and prediction performance.

Acknowledgment

This research work is a form of support for the acceleration of the new and renewable energy mix to the Government of Indonesia in accordance with the Decree on Energy Resources and Human Resources (ESDM) No. 188 of 2021 related to the use of biomass cofiring in coal-fired power plants and at the same time as an effort to support the target of the net zero emission 2060 program.

References

[1] B. N. Madanayake, S. Gan, C. Eastwick, and H. K. Ng, "Biomass as an energy source in coal co-firing and its feasibility enhancement via pre-treatment techniques," Fuel Process. Technol., vol. 159, pp. 287– 305, 2017, doi: 10.1016/j.fuproc.2017.01.029.

[2] PLN, "Rencana Usaha Penyediaan Tenaga Listrik (RUPTL) PT PLN (Persero) 2021-2030.," Rencana Usaha Penyediaan Tenaga List. 2021-2030, pp. 2019–2028, 2021. ("(PDF) Tantangan dan Peluang Pembangunan Proyek Pembangkit Listrik ...")

[3] K. Nowak and S. Rabczak, "Co-combustion of biomass with coal in grate water boilers at low load boiler operation," Energies, vol. 14, no. 9, 2021, doi: 10.3390/en14092520.

[4] Hariana, Prabowo, E. Hilmawan, F. Milky Kuswa, A. Darmawan, and M. Aziz, "A comprehensive evaluation of cofiring biomass with coal and slagging-fouling tendency in pulverized coal-fired boilers," Ain Shams Eng. J., vol. 14, no. 7, p. 102001, 2023, doi: 10.1016/j.asej.2022.102001.

[5] Y. Jeong et al., "Investigation and Optimization of Co-Combustion Efficiency of Food Waste Biochar and Coal," Sustain., vol. 15, no. 19, 2023, doi: 10.3390/su151914596.

[6] M. Soleh, A. H. Ahmad, F. B. Juangsa, P. S. Darmanto, and A. D. Pasek, "Impact of different kinds of biomass mixtures on combustion performance, interaction and synergistic effects in cofiring of coal and biomass in steam power plants," Clean Energy, vol. 7, no. 5, pp. 1136–1147, 2023, doi: 10.1093/ce/zkad049.

[7] J. H. Chow and J. J. Sanchez-Gasca, "Turbine-Governor Models and Frequency Control," in Power System Modeling, Computation, and Control, 2019, pp. 327–370. doi: 10.1002/9781119546924.ch12.

[8] A. Arastou, H. Rabieyan, and M. Karrari, "Inclusive modelling and

parameter estimation of a steam power plant using an LMI-based unknown input reconstruction algorithm," IET Gener. Transm. Distrib., vol. 16, no. 7, pp. 1425–1437, 2022, doi: 10.1049/gtd2.12379.
[9] F. S. Abdullah, A. N. Hamoodi, and R. A. Mohammed, "Performance Improvement in Steam Turbine in Thermal Power Plants Using Artificial Neural Network," J. Eur. des Syst. Autom., vol. 54, no. 6, pp. 891–895, 2021, doi: 10.18280/jesa.540611.
[10] N. Nahak, S. Satapathy, J. Samal, and S. K. Swain, "Optimal fractional steam governor damping controller with variable solar penetrations," Mater. Today Proc., vol. 74, pp. 895–900, 2023, doi: 10.1016/j.matpr.2022.11.290.
[11] C. Mishra and D. L. Gupta, "Deep Machine Learning and Neural Networks: An Overview," IAES Int. J. Artif. Intell., vol. 6, no. 2, p. 66, 2017, doi: 10.11591/ijai.v6.i2.pp66-73.
[12] C. Arthur, N. Yudistira, and C. Dewi, "AutoCyclic: Deep Learning Optimizer for Time Series Data Prediction," IEEE Access, vol. 12, no. December 2023, pp. 14014–14026, 2024, doi: 10.1109/ACCESS.2024.3356553.
[13] A. W. Wiranata and D. A. Asfani, "The Prediction and Operational Control System of the Cofiring Combined Cycle Power Plant Using Deep Learning Methods to Improve Power Generation Performance," ICT-PEP 2024 - Int. Conf. Technol. Policy Energy Electr. Power Resilient Power Syst. Navig. Clean Energy Transition, Proc., pp. 324– 329, 2024, doi: 10.1109/ICT-PEP63827.2024.10733418.
[14] H. Dwi Rizqi et al., "Kajian Potensi Bambu untuk Mendukung Penerapan Co-firing pada Pembangkit Listrik Jawa Bali," Pengabdi. Kpd. Masy., vol. 7, no. 1, pp. 2613–9960, 2023, [Online]. Available: https://doi.org/10.12962/j26139960.v7i1.277
[15] M. F. Ilham and S. W. A. Suedy, "Effect of Cofiring Using Sawdust on Steam Coal Power Plant Heat Rate Value," J. Energi Baru dan Terbarukan, vol. 3, no. 2, pp. 121–127, 2022, doi: 10.14710/jebt.2022.13828.
[16] Q. Wang, X. Wang, and R. Li, "Does urbanization redefine the environmental Kuznets curve? An empirical analysis of 134 Countries," Sustain. Cities Soc., vol. 76, p. 103382, Jan. 2022, doi: 10.1016/j.scs.2021.103382.
[17] Q. Li, D. Li, K. Zhao, L. Wang, and K. Wang, "State of health estimation of lithium-ion battery based on improved ant lion optimization and support vector regression," J. Energy Storage, vol. 50, p. 104215, Jun. 2022, doi: 10.1016/J.EST.2022.104215.
[18] A. Kaveh and N. Khavaninzadeh, "Efficient training of two ANNs using four meta-heuristic algorithms for predicting the FRP strength," Structures, vol. 52, pp. 256–272, Jun. 2023, doi: 10.1016/J.ISTRUC.2023.03.178.
[19] W. Jian et al., "SA-Bi-LSTM: Self Attention with Bi-Directional LSTM-Based Intelligent Model for Accurate Fake News Detection to Ensured Information Integrity on Social Media Platforms," IEEE Access, vol. 12, no. April, pp. 48436–48452, 2024, doi: 10.1109/ACCESS.2024.3382832.
[20] K. Khan et al., "Data-driven green energy extraction: Machine learning-based MPPT control with efficient fault detection method for the hybrid PV-TEG system," Energy Reports, vol. 9, pp. 3604–3623, 2023, doi: 10.1016/j.egyr.2023.02.047.
[21] T. Falconer and L. Mones, "Leveraging Power Grid Topology in Machine Learning Assisted Optimal Power Flow," IEEE Trans. Power Syst., vol. 38, no. 3, pp. 2234–2246, 2023, doi: 10.1109/TPWRS.2022.3187218.
[22] Y. Wang, Z. Xiao, and G. Cao, "A convolutional neural network method based on Adam optimizer with power-exponential learning rate for bearing fault diagnosis," J. Vibroengineering, vol. 24, no. 4, pp. 666–678, 2022, doi: 10.21595/jve.2022.22271.
[23] S. Liao, X. Jiang, and Z. Ge, "Weakly Supervised Multilayer Perceptron for Industrial Fault Classification With Inaccurate and Incomplete Labels," IEEE Trans. Autom. ("Xiaoyu Jiang - Google Scholar") ("Xiaoyu Jiang - Google Scholar") Sci. Eng., vol. 19, no. 2, pp. 1192–1201, 2022, doi: 10.1109/TASE.2020.3043531.
[24] Y. Choi, X. Shao, and H. S. Hwang, "Highly Accurate Short-Term Gas Consumption and Elapsed Time Forecasting Using Multi-Channel Deep Neural Network," IEEE Access, vol. 9, pp. 157447–157457, 2021, doi: 10.1109/ACCESS.2021.3129601.
[25] X. Chen, L. Gupta, and S. Tragoudas, "Improving the Forecasting and Classification of Extreme Events in Imbalanced Time Series Through Block Resampling in the Joint Predictor-Forecast Space," IEEE Access, vol. 10, no. November, pp. 121048–121079, 2022, doi: 10.1109/ACCESS.2022.3219832.
[26] R. Chandra, "Evaluation of Deep Learning Models for Multi-Step Ahead Time Series Prediction," IEEE Access, vol. 9, pp. 83105– 83123, 2021, doi: 10.1109/ACCESS.2021.3085085.
[27] Z. Peng, C. Zhang, and Y. Tian, "Crude Oil Price Time Series Forecasting: A Novel Approach Based on Variational Mode Decomposition, Time-Series Imaging, and Deep Learning," vol. 11, no. July 2023.
[28] N. Buduma, N. Buduma, and J. Papa, Oreilly.Fundamentals.of. Deep.Learning.Designing.Next-Generation.Machine. Intelligence. Algorithms. 2nd.Edition. Jun.2022.
[29] D. Li, X. Wang, J. Sun, and Y. Feng, "Radial Basis Function Neural Network Model for Dissolved Oxygen Concentration Prediction Based on an Enhanced Clustering Algorithm and Adam," IEEE Access, vol. 9, pp. 44521–44533, 2021, doi: 10.1109/ACCESS.2021.3066499.
[30] J. Hong, J. Park, and S. Park, "StackDA: A Stacked Dual Attention Neural Network for Multivariate Time-Series Forecasting," IEEE Access, vol. 9, pp. 145955–145967, 2021, doi: 10.1109/ACCESS.2021.3122910.
[31] R. H. Karlsen et al., "Examining 3-month test-retest reliability and reliable change using the Cambridge Neuropsychological Test Automated Battery," Appl. Neuropsychol., vol. 29, no. 2, pp. 146–154, 2022, doi: 10.1080/23279095.2020.1722126.